Preparation of Mesoporous Fe$_2$O$_3$-Supported ZSM-5 Zeolites by Carbon-Templating and their Evaluation as Photo-Fenton Catalysts to Degrade Organic Pollutant

Jivago Schumacher de Oliveira[a], Marcio Antonio Mazutti[a], Ernesto Antonio Urquieta-González[b],

Edson Luiz Foletto[a]*, Sérgio Luiz Jahn[a]

[a] *Department of Chemical Engineering, Federal University of Santa Maria, 97105-900, Santa Maria, RS, Brazil*
[b] *Research Center on Advanced Materials and Energy, Federal University of São Carlos, C. Postal 676, 13565-905, São Carlos, SP, Brazil*

Mesoporous Fe$_2$O$_3$-supported ZSM-5 zeolites were prepared by carbon-templating and subsequently evaluated as photo-Fenton catalysts to degrade a dye used as a model heavy organic pollutant. The synthesis procedure of the mesoporous ZSM-5 zeolites was performed employing a nucleating gel and carbon particles as mesopores template. Thereafter, the precursor salt of the iron oxide (Fe$_2$O$_3$) was impregnated and then calcined to obtain the final catalyst. For comparison purposes, a conventional Fe$_2$O$_3$-supported ZSM-5 zeolite was also prepared. The results showed that the amount of intracrystalline mesopores formed in the ZSM-5 crystals was influenced by the amount of carbon added into the synthesis mixture. In comparison to the conventional prepared catalyst, the mesoporous Fe$_2$O$_3$/ZSM-5 ones showed an improved performance in the degradation of the target organic pollutant by the photo-Fenton reaction, which was attributed to the improvement of their textural properties as consequence of the mesopores generation.

Keywords: *Mesoporous ZSM-5, carbon template, Fe$_2$O$_3$-supported ZSM-5, photo-Fenton reaction, dye degradation*

1. Introduction

Heterogeneous photo-Fenton reaction has proved to be an emerging and promising technology for remediation of organic pollutant containing in liquid industrial effluents[1,2]. The technique consist in the use of iron-based catalysts which, in contact with hydrogen peroxide, and in the presence of light irradiation, produce highly oxidative radicals (HO$^•$) in aqueous solution[3], leading to degradation of organic molecules. The iron-based catalysts can be directly used in the chemical reaction in the form of finely divided powders or immobilized on solid supports[4]. Several works have demonstrated that the use of different supports to disperse iron oxides lead to greater efficiency in catalytic oxidation processes[5-7]. Among the various available supports, ZSM-5 zeolite has been widely used as catalyst support in Fenton oxidation systems due to their intrinsic properties such as thermal stability, high surface area, and uniform pores and channels[8-10]. However, the catalytic efficiency of ZSM-5 zeolite may be severely limited due to their microporous nature, which restricts the access of reactant molecules to active catalyst sites located inside of the zeolite crystals[11,12]. Due to this fact, the preparation of mesoporous ZSM-5 zeolites has attracted a great interest in the catalytic applications[13-15]. Among the several methods showed in the literature to produce mesoporous zeolites[16-19], the carbon-templating method has demonstrated to be relatively facile and inexpensive, being that after burning of the carbon particles, zeolite crystals with intracrystalline mesoporous are obtained[16,20,21]. However, works reporting the preparation of m*esoporous* Fe$_2$O$_3$-supported ZSM-5 zeolites employing a nucleating gel and carbon particles as mesopores template in the synthesis procedure for application as photo-Fenton catalyst under visible light has not been reported yet.

Hence, this work aimed to synthesize mesoporous ZSM-5 zeolites using a nucleating gel and carbon particles as mesopores template. The obtained mesoporous ZSM-5 samples were impregnated with the precursor iron salt, being subsequently calcined to obtain the Fe$_2$O$_3$-supported *ZSM-5* catalysts, which were evaluated in the photo-Fenton degradation of a dye molecule used as a model organic pollutant. In addition, the effect of the amount of nucleating gel as well as the amount of carbon particles added into the synthesis mixture on the textural properties of the obtained mesoporous ZSM-5 zeolites was also investigated.

2. Materials and methods

2.1. Preparation of mesoporous ZSM-5 zeolites

The used reagents were: sodium silicate (Na$_2$SiO$_3$, 53 %wt. Na$_2$O, 47 %wt. SiO$_2$, Sigma-Aldrich), tetrapropylammonium hydroxide (TPAOH, 20 %v/v, Sigma-Aldrich), aluminum

sulfate [(Al$_2$(SO$_4$)$_3$, Sigma-Aldrich], deionized water, sulfuric acid, 95% (Vetec), fumed silica (Sigma-Aldrich, 200 m^2 g^{-1}).

The nucleating gel was prepared following the procedure described in a previous work[22], that resulted in a mixture with a molar composition of: 1 SiO$_2$: 0.3 Na$_2$O: 0.05 TPA$_2$O: 24 H$_2$O: 0.3 OH$^-$. Then, the mixture was charged into a PTFE-lined stainless autoclave, and aged for 7 days at 60 °C. The precursor gel for the synthesis of the Na-ZSM-5 zeolites was prepared using the molar composition of: 1 SiO$_2$: 0.033 Al$_2$O$_3$: 0.3 Na$_2$O: 25 H$_2$O: 0.25 OH$^-$. Then, different amounts of the nucleating gel (1, 2.5 or 5 % wt.) were added into the precursor gel, resulting in the ratios of TPAOH/ SiO$_2$ = 0.001, 0.0025 and 0.005, respectively. The respective mixtures were charged into PTFE-lined stainless autoclaves and submitted to a hydrothermal treatment at 170 °C for 12 h. After the crystallization process, the powders were washed with deionized water and then dried at 110 °C for 24 h. After analyzing the results shown in Figure 1, where the use of different concentrations of nucleating gel did not result in significant changes in the formation of the obtained ZSM-5 zeolites, it was chosen the mixture having 1 % wt. of SiO$_2$ for the subsequent preparation of the mesoporous ZSM-5 samples. The procedure described above has as advantage of the use of low amount of TPAOH, which is an expensive reagent in the synthesis of ZSM-5 zeolites[22].
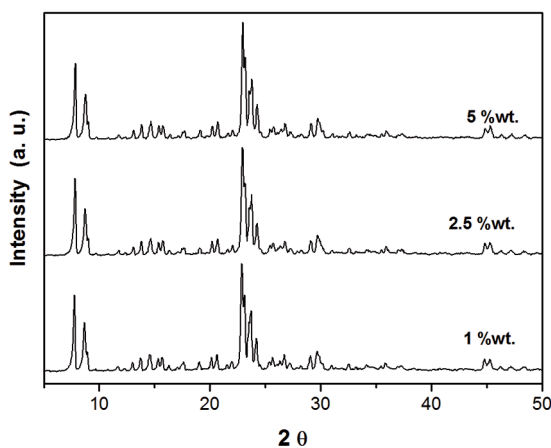
Figure 1: X-ray diffratograms of ZSM-5 samples prepared with different concentrations of nucleating gel.

Then, different amounts of carbon black (Black Pearls®2000, Cabot Corporation) were added into the precursor gel in order to generate the following carbon/silica (C/SiO$_2$) ratios: 0, 0.125, 0.25, 0.5, 1.0 and 2.0. The respective samples were named as ZP, ZC1, ZC2, ZC3, ZC4, ZC5, where ZP corresponds to sample synthesized without carbon particles. The resulting mixture was homogenized during 30 min using an ultrasound equipment. Subsequently, the respective mixture was charged into PTFE-lined stainless autoclaves and submitted to a hydrothermal treatment at 170 °C for 12 h. After the crystallization step, the formed powders were

vacuum filtered, washed with deionized water and then dried at 110 °C for 24 h. Finally, the occluded carbon black was removed by calcination at 600 °C during 10 h under oxidizing atmosphere.

2.2. Preparation of mesoporous Fe$_2$O$_3$-supported ZSM-5 zeolites

The mesoporous Fe$_2$O$_3$-supported ZSM-5 zeolites were prepared by wet impregnation, using a procedure described in a previously published work[23], which involves three stages: impregnation, dispersion and heat treatment. The impregnation step was performed by adding 30 mL per gram of zeolite of an aqueous solution of iron salt in isopropyl alcohol per gram of zeolite, in order to result in a sample containing 7 wt. % of Fe$_2$O$_3$. Subsequently, the suspension was submitted to an ultrasound process (Bransonic Ultrasonic Cleaner 2510R-MT - 100 W, 42 KHz ± 6) at 60 °C for 40 min, in order to promote the dispersion of iron on the ZSM-5 particles and simultaneously to promote the solvent evaporation. Then, the formed solids were submitted to a heat treatment at 250 °C for 4 h under oxidizing atmosphere. The obtained samples were named ZP-Fe, ZC1-Fe, ZC2-Fe, ZC3-Fe, ZC4-Fe and ZC5-Fe, where ZP-Fe corresponds to the ZSM-5 sample prepared without the presence of carbon particles.

2.3. Characterization

The samples were characterized by X-ray diffraction (XRD) using a Rigaku Miniflex model 300 diffractometer being operated with Cu-Kα radiation (λ = 1.5418 Å), 30 kV, 10 mA, step size of 0.03º and a count time of 0.5 s per step. The textural properties were determined using a Micromeritics ASAP 2020 apparatus. The morphology and chemical analysis of the samples were obtained by scanning electron microscopy (SEM) using a FEI Inspect S 50 apparatus coupled to an auxiliary Energy Dispersive X-ray Spectroscopy (EDS) detector. For the EDS analysis, the powder samples were put onto the sample holder, which was isolated by a carbon tape. In order to observe the dispersion of Fe$_2$O$_3$ particles on the support (ZC5-Fe sample), a SEM analysis was done using a Philips XL 30 FEG instrument operated at 25 kV with a secondary electron detector. The sample was suspended in acetone (99.5 vol %) by sonication and the suspension was dropped on a metal grid. Previous to the analysis, a thin coating of gold was deposited onto the sample.

2.4. Catalytic evaluation

For the photo-Fenton assays, a dye (CI: Reactive Red 141 dye, CAS number 61931-52-0; chemical formula is C$_{52}$H$_{34}$O$_{26}$S$_8$Cl$_{12}$N$_{14}$; molecular weight = 1,952 g mol^{-1}; average molecular size of 2.3 nm [24]) was used as a model organic

Preparation of Mesoporous Fe₂O₃-Supported ZSM-5 Zeolites by Carbon-Templating and their Evaluation as Photo-Fenton Catalysts to Degrade Organic Pollutant

1401

molecule, which it is widely applied in textile industries. The experimental conditions used in the experiments were based on a previous work[25]. The experiments were carried out at 25 °C using a glass reactor with 0.25 L of capacity. The irradiation was provided by a commercial fluorescent lamp (EMPALUX, 85 W, luminous efficacy of irradiation = 65 lumens/W, emission at wavelength above 400 nm) fixed 10 cm above the aqueous dye solution. In a typical experiment, the reactor was charged with 100 mL of solution containing an initial dye concentration of 50 mg L^{-1}, at pH adjusted at 3.0, employing an aqueous solution of sulfuric acid 0.1 mol L^{-1}, under *continuous magnetic stirring*. After addition of the catalyst (0.5 g L^{-1}), the medium was maintained under stirring for 60 min without irradiation, in order to reach the adsorption equilibrium. Subsequently, the suspension was irradiated by the lamp and the hydrogen peroxide (8 mM) was added to initiate the reaction. Samples were withdrawn using a syringe attached to a filter (PVDF membrane, 0.45 µm). The dye concentration was determined using a UV-Vis spectrophotometer (Bel Photonics, SP1105), with a maximum wavelength of 543 nm. Decolorization efficiency (*DE*, %) was determined by the following equation: DE (%) = $[(A_0 - A_t)/A_0] \times 100$, where: A_t is the absorbance after a reaction time *t*, and A_0 is the initial absorbance before the reaction.

Catalytic assays were also performed to evaluate the conventional Fenton reaction (without irradiation), and also with the system under visible light irradiation, but without the presence of catalyst. The stability of the catalysts was evaluated by determination of the iron-leached amount in the reaction media after the photo-Fenton degradation, which was measured by atomic absorption spectroscopy (Agilent Technologies, 200 series AA).

3. Results and discussion

3.1. Characterization

In Figure 1 are illustrated the X-ray diffractograms (XRD) of the ZSM-5 samples prepared with different amounts of nucleating gel related to the fixed concentration of the precursor gel. It can be observed that all the analyzed samples show the characteristic peaks of the MFI type structure[26,27], confirming the formation of the ZSM-5 zeolite. In addition, it is observed that the peaks intensity of the samples is very similar, indicating that the different concentrations of the nucleating gel used in this study did not influenced the crystallinity of the obtained ZSM-5 zeolites. Therefore, the lower content of nucleating gel (that resulted in a value of 1 wt. % of SiO_2) was chosen for the subsequent preparation of ZSM-5 samples with different carbon amounts in the synthesis mixture (Figure 2).

Figure 2 shows the XRD patterns of the samples synthesized without and in the presence of different amounts of carbon particles. It can be seen that the crystalline phase
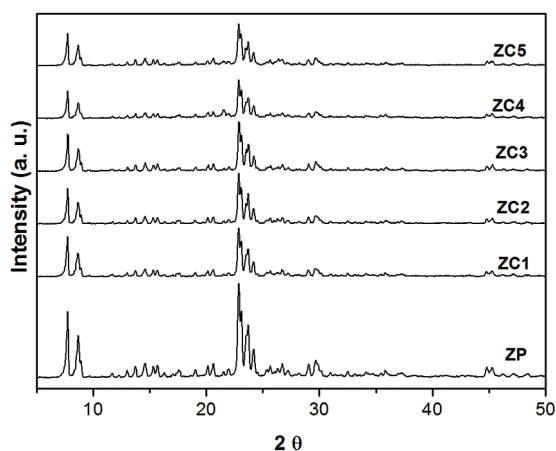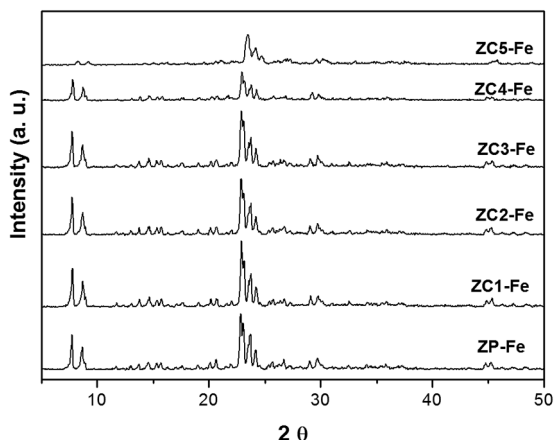

Figure 2: X-ray diffratograms of ZSM-5 samples prepared with different concentrations of carbon particles and sample prepared without the presence of carbon (ZP sample).

corresponding to the MFI structure is observed for all the obtained samples. However, it is observed that the intensity of the XRD peaks decreases with the increasing of the carbon amount used in the synthesis, resulting in a gradual decrease of the relative crystallinity, whose values (shown in Table 1) were calculated according to a previous work[28], using the ZP sample as reference. These results demonstrate that the carbon presence influences the crystallization process of the ZSM-5 structure. Similar behavior has been found by other researchers[16,21]. It is important to notice that the SiO_2/Al_2O_3 ratio of the conventional ZP sample was 31.5 and remained practically unchanged for samples synthesized in the presence of different amounts of carbon particles (Table 1).

Table 1: Relative crystallinity and SiO_2/Al_2O_3 ratio of ZSM-5 samples.
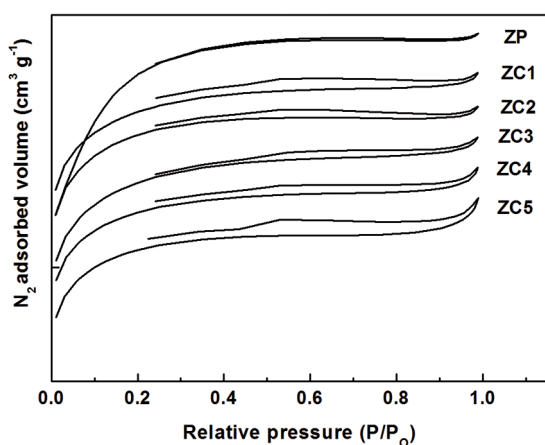
Sample	Crystallinity degree (%)	SiO_2/Al_2O_3 ratio
ZP	100	31
ZC1	90	30
ZC2	91	31
ZC3	91	30
ZC4	78	30
ZC5	75	31

The X-ray diffractograms shown in Figure 3 correspond to the prepared Fe₂O₃-supported ZSM-5 zeolites. As can be evidenced, no peaks corresponding to the presence of Fe_2O_3 can be identified in the diffractograms, indicating that this component must be present as very small particles highly dispersed on the support. These findings are consistent with other previously reported works[29,30]. From Figure 3, it is also noticed that no important difference appear in the zeolite diffractograms after the impregnation process. The amount of Fe_2O_3 impregnated on ZSM-5 was about 7 wt. % for all the prepared samples, which was confirmed by EDS analysis (not shown).
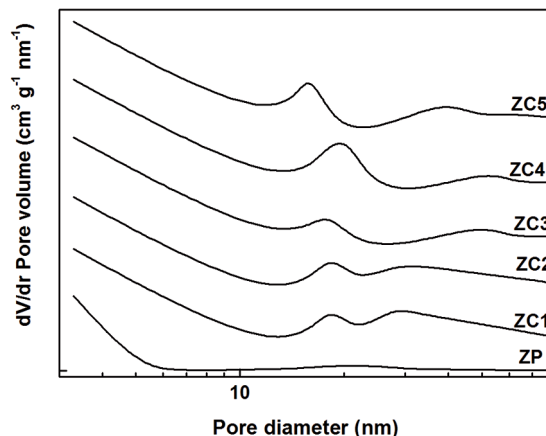
Figure 3: X-ray diffratograms of ZSM-5 samples prepared with different concentrations of carbon particles and impregnated with 7 wt. % of Fe_2O_3. ZP-Fe: sample prepared without carbon and also impregnated with 7 wt. % of Fe_2O_3.

Figure 5: Pore size distribution plots of ZSM-5 zeolites synthesized with different concentrations of carbon particles (Log scale graph). ZP: sample prepared without carbon.

Figure 4 shows the nitrogen adsorption–desorption isotherms for the obtained zeolites. It can be observed that the isotherms of the ZSM-5 zeolite synthesized without the addition of carbon (ZP sample) can be categorized as type I, according to the International Union of Pure and Applied Chemistry (IUPAC) classification, showing a greater pore volume variation at lower relative pressures ($P/P_0 < 0.4$) and without hysteresis loop, characteristic of microporous materials. On the other hand, the ZSM-5 samples synthesized in the presence of carbon particles exhibit a combination of type I and type IV isotherms with H2 hysteresis loop, characteristic of solids having microporous and mesoporous structure[31,32].

Figure 4: N_2 adsorption–desorption isotherms of ZSM-5 zeolites synthesized with different concentrations of carbon particles. ZP: sample prepared without carbon.

The corresponding pore size distribution curves (Figure 5) were measured from the adsorption branches of the isotherms according to the Barrett–Joyner–Halenda (BJH) method. It can be seen that the ZSM-5 zeolites synthesized in the presence of carbon particles display a broader pore size distribution compared to sample prepared without the addition of carbon (ZP sample), with a highest peak centered in the mesoporous region (between 15 and 23 nm). In addition, a smaller peak can be observed along the mesoporous region, revealing a material with a bimodal pore size distribution[33]. These features are of great importance for catalytic purposes because it allows greater accessibility and diffusion of large molecules within the zeolite pores.

In order to better analyze the formation of mesoporous ZSM-5 zeolites employing a nucleating gel and carbon particles as mesopores template, the textural properties are shown in Table 2. As can be observed, a slight increase occurs in the specific surface area of the samples synthesized in the presence of carbon compared to the conventional ZP sample. From Figure 6, it can be also observed that an increase in the C/SiO_2 ratio results in a decrease of the micropores volume and as expected in an increase of the mesopores volume. In addition, all the ZSM-5 samples maintained high values of the BET area, total porous volume and mesopores volume after the impregnation with iron. The values of specific surface area (BET) and pore volume obtained in this work are similar to those ones published by others researchers[18,21,34], using carbon nanoparticles as mesopores template for the ZSM-5 synthesis.

Figure 7 shows SEM images of samples ZP-Fe (Figure 7a), ZC4-Fe (Figure 7b), ZC5-Fe (Figure 7c) and the distribution of Fe_2O_3 particles on the ZC5-Fe sample (Figure 7d). All samples exhibit similar zeolite particle shapes, demonstrating that the use of carbon black in the synthesis of ZSM-5 had no significant effect on this characteristic. In addition, the particle size for all the obtained ZSM-5 zeolites was practically the same, around 5 μm. From Figure 7d, it is possible to observe a good dispersion of Fe_2O_3 particles on the support.

Preparation of Mesoporous Fe$_2$O$_3$-Supported ZSM-5 Zeolites by Carbon-Templating and their Evaluation as Photo-Fenton Catalysts to Degrade Organic Pollutant

1403

Table 2: Physical properties of ZSM-5 samples.

Sample	C/SiO$_2$ ratio	Surface area (m^2 g^{-1})			Pore volume (cm^3 g^{-1})		
		BET	Microporous	Externa	Total	Micropores	Mesopores
ZP	0	264	229	35	0.1451	0.1445	0.0006
ZC1	0.125	283	246	37	0.1586	0.1296	0.0290
ZC2	0.25	298	258	39	0.1693	0.1300	0.0393
ZC3	0.5	286	248	39	0.1655	0.1249	0.0406
ZC4	1	273	237	36	0.1597	0.0899	0.0698
ZC5	2	270	235	35	0.1573	0.0937	0.0636
ZP-Fe	0	224	164	60	0.1217	0.1207	0.0126
ZC1-Fe	0.125	280	218	62	0.1516	0.1019	0.0497
ZC2-Fe	0.25	268	210	58	0.1508	0.0955	0.0553
ZC3-Fe	0.5	252	202	49	0.1492	0.0895	0.0597
ZC4-Fe	1	248	190	59	0.1519	0.06905	0.0829
ZC5-Fe	2	234	184	50	0.1488	0.07014	0.0786
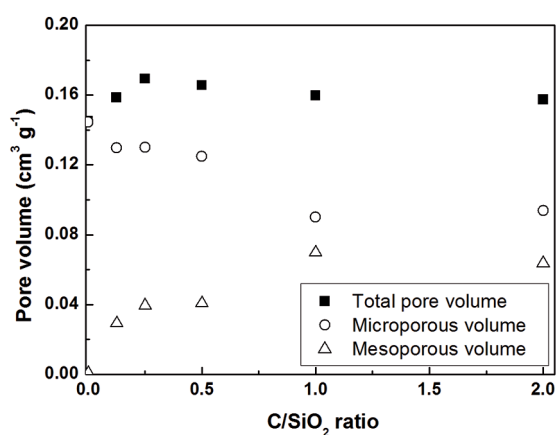
Figure 6: Influence of the C/SiO$_2$ ratio employed in the synthesis gel on the microporous and mesoporous volume of the zeolites.
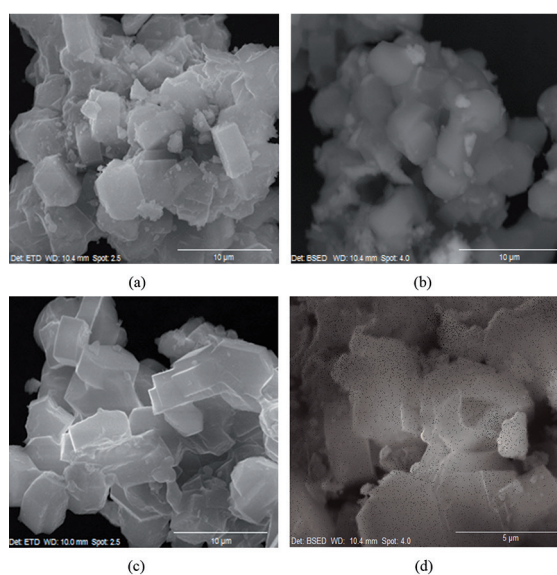
Figure 7: SEM images of samples: (a) ZP-Fe (magnification: 10,000 X), (b) ZC4-Fe (magnification: 10,000 X), (c) ZC5-Fe (magnification: 10,000 X) and (d) distribution of Fe$_2$O$_3$ particles on the ZC5-Fe sample (magnification: 30,000 X).

3.2. Catalytic evaluation

The activity of mesoporous Fe$_2$O$_3$-supported ZSM-5 catalysts for the decolorization of the target dye molecule as a function of the reaction time is shown in Figure 8. The catalytic activity of the samples in the conventional Fenton process (without light irradiation) and the dye degradation without the presence of catalyst (with light irradiation) were also evaluated and the decolorization results were below of 17 and 5 %, respectively. However, as can be seen from Figure 8 significant decolorization was obtained with the employ of the photo-Fenton process. With the conventional ZP-Fe sample it was reached 80 % of decolorization for a reaction time of 60 min, whereas the ZSM-5 zeolites synthesized using the mesopores template (carbon black) showed superior degradation efficiency, behavior that it is attributed to the presence of intracrystalline mesoporosity (Table 2) that improved the diffusion of the dye molecules. Furthermore, the ZC4-Fe sample showed the highest efficiency, with total decolorization at 60 min, due to the presence of the highest mesoporous volume (Table 2) that may have contributed to a better dispersion of the active phase. As mentioned, the superior catalytic behaviour of the Fe$_2$O$_3$-supported-ZSM-5 catalysts synthesized in the presence of carbon particles is clearly understood from the improved diffusion of the big dye molecule (2.30 nm[24]) in the created mesopores with mean diameter of about 20 nm. Thus the ratio between the mesopore diameter and the dye molecular size is 8.6. So this implies that the mesopore diameter of the catalyst could accommodate about eight dye molecules, and therefore, favoring to a high catalytic activity.

For comparison purposes regarding to the catalytic activity aiming the degradation of the Reactive Red 141 dye used in this study, some catalysts have been used and reported in the literature. Stringhini et al.[35] observed a total dye removal at 120 min of reaction using ZnAl$_2$O$_4$ catalyst under UV irradiation, whereas Foletto et al.[24] obtained
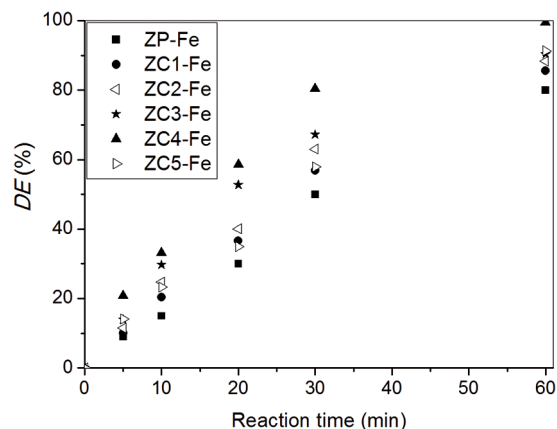
Figure 8: Decolorization efficiency (*DE*, %) of ZSM-5 samples prepared with different concentrations of carbon particles and impregnated with 7 wt. % of Fe_2O_3. ZP-Fe: sample prepared without carbon and also impregnated with 7 wt. % of Fe_2O_3.

total removal at 180 min using the same catalyst, but under sunlight. $ZnFe_2O_4$ catalyst prepared by microwave irradiation showed 90% of dye removal at 60 min of reaction under visible light[36]. Therefore, the results obtained in this work demonstrate that the mesoporous Fe_2O_3-supported ZSM-5 zeolites are efficient catalysts for the removal of Reactive Red 141 dye from aqueous solution.

Moreover, in order to evaluate the stability of the catalysts, the iron-leached amount in the solution after reaction was determined, resulting in a value below of 1 mg L^{-1} for all the studied catalysts. According to the Brazilian environmental legislation[37], the value for iron disposal in effluents is 15 mg L^{-1}. This result indicates a satisfactory stability of the prepared Fe_2O_3-supported ZSM-5 zeolites for the use as catalyst in heterogeneous photo-Fenton reactions for degradation of organic pollutants, such as dyes present in industrial wastewaters.

4. Conclusions

The technique employing nucleating gel and carbon particles as mesopores template was very promising for the production of microporous-mesoporous ZSM-5 zeolites. Different nucleating gel concentrations used in this work had no effect in the formation of the ZSM-5 zeolite structure. Increasing the amount of carbon particles used in the synthesis of ZSM-5 resulted in a decrease of the micropores volume and, as expected, in an increase in the mesopores volume. The mesoporous Fe_2O_3-supported ZSM-5 zeolites showed higher photo-Fenton activity to degrade the Reactive Red 141 dye compared to the conventional Fe_2O_3-supported ZSM-5 zeolite. Therefore, the studied Fe_2O_3-supported ZSM-5 zeolites possessing a microporous-mesoporous structure are promising catalysts to degrade organic pollutants in industrial wastewaters.

6. References

1. Anchieta CG, Severo EC, Rigo C, Mazutti MA, Kuhn RC, Muller EI, et al. Rapid and facile preparation of zinc ferrite ($ZnFe_2O_4$) oxide by microwave-solvothermal technique and its catalytic activity in heterogeneous photo-Fenton reaction. *Materials Chemistry and Physics*. 2015;160:141-147. http://dx.doi.org/10.1016/j.matchemphys.2015.04.016

2. Severo EC, Anchieta CG, Foletto VS, Kuhn RC, Collazzo GC, Mazutti MA, et al. Degradation of Amaranth azo dye in water by heterogeneous photo-Fenton process using $FeWO_4$ catalyst prepared by microwave irradiation. *Water Science and Technology*. 2016;73(1):88-94. http://dx.doi.org/10.2166/wst.2015.469

3. Pignatello JJ. Dark and photoassisted iron[(3+)]-catalyzed degradation of chlorophenoxy herbicides by hydrogen peroxide. *Environmental Science & Technology*. 1992;26(5):944-951. http://dx.doi.org/10.1021/es00029a012

4. Zhuang H, Han H, Ma W, Hou B, Jia S, Zhao Q. Advanced treatment of biologically pretreated coal gasification wastewater by a novel heterogeneous Fenton oxidation process. *Journal of Environmental Sciences*. 2015;27:12-20. http://dx.doi.org/10.1016/j.jes.2014.12.015

5. Gao Y, Wang Y, Zhang H. Removal of Rhodamine B with Fe-supported bentonite as heterogeneous photo-Fenton catalyst under visible irradiation. *Applied Catalysis B: Environmental*. 2015;178:29-36. http://dx.doi.org/10.1016/j.apcatb.2014.11.005

6. Su CC, Fan CC, Anotai J, Lu MC. Effect of the iron oxide catalyst on o-toluidine oxidation by the fluidized-bed Fenton process. *Environmental Technology*. 2014;35(1-4):89-94. http://dx.doi.org/10.1080/09593330.2013.811543

7. Yuan N, Zhang G, Guo S, Wan Z. Enhanced ultrasound-assisted degradation of methyl orange and metronidazole by rectorite-supported nanoscale zero-valent iron. *Ultrasonics Sonochemistry*. 2016;28:62-68. http://dx.doi.org/10.1016/j.ultsonch.2015.06.029

8. Cihanoğlu A, Gündüz G, Dükkanci M. Degradation of acetic acid by heterogeneous Fenton-like oxidation over iron-containing ZSM-5 zeolites. *Applied Catalysis B: Environmental*. 2015;165:687-699. http://dx.doi.org/10.1016/j.apcatb.2014.10.073

9. Gonzalez-Olmos R, Martin MJ, Georgi A, Kopinke FD, Oller I, Malato S. Fe-zeolites as heterogeneous catalysts in solar Fenton-like reactions at neutral pH. *Applied Catalysis B: Environmental*. 2012;125:51-58. http://dx.doi.org/10.1016/j.apcatb.2012.05.022

10. Queirós S, Morais V, Rodrigues CSD, Maldonado-Hódar FJ, Madeira LM. Heterogeneous Fenton's oxidation using Fe/ZSM-5 as catalyst in a continuous stirred tank reactor. *Separation and Purification Technology*. 2015;141:235-245. http://dx.doi.org/10.1016/j.seppur.2014.11.046

Preparation of Mesoporous Fe$_2$O$_3$-Supported ZSM-5 Zeolites by Carbon-Templating and their Evaluation as
Photo-Fenton Catalysts to Degrade Organic Pollutant

1405

11. Wei X, Smirniotis PG. Development and characterization of mesoporosity in ZSM-12 by desilication. *Microporous and Mesoporous Materials*. 2006;97(1-3):97-106. http://dx.doi.org/10.1016/j.micromeso.2006.01.024

12. Sashkina KA, Parkhomchuk EV, Rudina NA, Parmon VN. The role of zeolite Fe-ZSM-5 porous structure for heterogeneous Fenton catalyst activity and stability. *Microporous and Mesoporous Materials*. 2014;189:181-188. http://dx.doi.org/10.1016/j.micromeso.2013.11.033

13. Sashkina KA, Labko VS, Rudina NA, Parmon VN, Parkhomchuk EV. Hierarchical zeolite FeZSM-5 as a heterogeneous Fenton-type catalyst. *Journal of Catalysis*. 2013;299:44-52. http://dx.doi.org/10.1016/j.jcat.2012.11.028

14. Pérez-Ramírez J, Verboekend D, Bonilla A, Abelló S. Zeolite catalysts with tunable hierarchy factor by pore-growth moderators. *Advanced Functional Materials*. 2009;19(24):3972-3979. http://dx.doi.org/10.1002/adfm.200901394

15. Fernandez C, Stan I, Gilson JP, Thomas K, Vicente A, Bonilla A, et al. Hierarchical ZSM-5 zeolites in shape-selective xylene isomerization: role of mesoporosity and acid site speciation. *Chemistry - A European Journal*. 2010;16(21):6224-6233. http://dx.doi.org/10.1002/chem.200903426

16. Chou YH, Cundy CS, Garforth AA, Zholobenko VL. Mesoporous ZSM-5 catalysts: Preparation, characterisation and catalytic properties. Part I: Comparison of different synthesis routes. *Microporous and Mesoporous Materials*. 2006;89(1-3):78-87. http://dx.doi.org/10.1016/j.micromeso.2005.10.014

17. Pérez-Ramirez J, Christensen CH, Egeblad K, Christensen CH, Groen JC. Hierarchical zeolites: enhanced utilisation of microporous crystals in catalysis by advances in materials design. *Chemical Society Reviews*. 2008;37(11):2530-2542. http://dx.doi.org/10.1039/B809030K

18. Tao Y, Kanoh H, Abrams L, Kaneko K. Mesopore-modified zeolites: preparation, characterization, and applications. *Chemical Reviews*. 2006;106(3):896-910. http://dx.doi.org/10.1021/cr040204o

19. Yu W, Deng L, Yuan P, Liu D, Yuan W, Chen F. Preparation of hierarchically porous diatomite/MFI-type zeolite composites and their performance for benzene adsorption: The effects of desilication. *Chemical Engineering Journal*. 2015;270:450-458. http://dx.doi.org/10.1016/j.cej.2015.02.065

20. Janssen AH, Schmidt I, Jacobsen CJH, Koster AJ, de Jong KP. Exploratory study of mesopore templating with carbon during zeolite synthesis. *Microporous and Mesoporous Materials*. 2003;65(1):59-75. http://dx.doi.org/10.1016/j.micromeso.2003.07.003

21. Koo JB, Jiang N, Saravanamurugan S, Bejblová M, Musilová Z, Čejka J, et al. Direct synthesis of carbon-templating mesoporous ZSM-5 using microwave heating. *Journal of Catalysis*. 2010;276(2):327-334. http://dx.doi.org/10.1016/j.jcat.2010.09.024

22. Stamires D, Lam YL, Gorne J, Wasserman R, Moreira Ferreira JC, Silva J, inventors; Albemarle Netherlands BV, assignee. *Nucleating gel, process for its preparation, and its use in the synthesis of MFI-type zeolite*. Patent Cooperation Treaty (PCT), no. WO/2006/087337. 2006 Aug 24. Available from: <http://patentscope.wipo.int/search/en/detail.jsf?docId=WO2006087337>. Access in: 4/10/2016.

23. Zamora RMR, Pérez AAM, Schouwenaars R, inventors; Universidad Nacional Autonoma de Mexico, assignee. *Process for producing a Fenton-type nanocatalyst of iron oxide nanoparticles supported in porous materials for the oxidation of pollutants present in water*. European Patent Office, no. MX2012000450. 2013 Feb 6. Available from: <http://worldwide.espacenet.com>. Access in: 4/10/2016.

24. Foletto EL, Battiston S, Simões JM, Bassaco MM, Pereira LSF, Flores EMM, et al. Synthesis of ZnAl$_2$O$_4$ nanoparticles by different routes and the effect of its pore size on the photocatalytic process. *Microporous and Mesoporous Materials*. 2012;163:29-33. http://dx.doi.org/10.1016/j.micromeso.2012.06.039

25. Anchieta CG, Cancelier A, Mazutti MA, Jahn SL, Kuhn RC, Gündel A, et al. Effects of solvent diols on the synthesis of ZnFe$_2$O$_4$ particles and their use as heterogeneous photo-Fenton catalysts. *Materials*. 2014;7(9):6281-6290. http://dx.doi.org/10.3390/ma7096281

26. Treacy MMJ, Higgins JB. *Collection of Simulated XRD Powder Patterns for Zeolites*, 4th Ed. The Structure Commission of the International Zeolite Association. New York: Elsevier; 2001. Available from: <http://www.iza-structure.org/databases/books/Collection_4ed.pdf>. Access in: 4/10/2016.

27. Pavlačková Z, Košová G, Žilková N, Zukal A, Čejka J. Formation of mesopores in ZSM-5 by carbon templating. *Studies in Surface Science and Catalysis*. 2006;162:905-912. http://dx.doi.org/10.1016/S0167-2991(06)80996-1

28. Foletto EL, Kuhnen NC, José HJ. Síntese da zeólita ZSM-5 e suas propriedades estruturais após troca iônica com cobre. *Cerâmica*. 2000;46(300):210-213. http://dx.doi.org/10.1590/S0366-69132000000400007

29. Zepeda TA, Pawelec B, Fierro JLG, Olivas A, Fuentes S, Halachev T. Effect of Al and Ti content in HMS material on the catalytic activity of NiMo and CoMo hydrotreating catalysts in the HDS of DBT. *Microporous and Mesoporous Materials*. 2008;111(1-3):157-170. http://dx.doi.org/10.1016/j.micromeso.2007.07.025

30. Wang A, Wang Y, Kabe T, Chen Y, Ishihara A, Qian W, et al. Hydrodesulfurization of dibenzothiophene over siliceous MCM-41-supported catalysts: II. Sulfided Ni–Mo catalysts. *Journal of Catalysis*. 2002;210(2):319-327. http://dx.doi.org/10.1006/jcat.2002.3674

31. Celzard A, Fierro V, Amaral-Labat G. Adsorption by Carbon Gels. In: *Tascón JMD, ed. Novel Carbon Adsorbents.* Chapter 7. Amsterdam: Elsevier; 2012. p. 207-244. http://dx.doi.org/10.1016/B978-0-08-097744-7.00007-7

32. Georgin J, Dotto GL, Mazutti MA, Foletto EL. Preparation of activated carbon from peanut shell by conventional pyrolysis and microwave irradiation-pyrolysis to remove organic dyes from aqueous solutions. *Journal of Environmental Chemical Engineering*. 2016;4(1):266-275. http://dx.doi.org/10.1016/j.jece.2015.11.018

33. Nuernberg GDB, Foletto EL, Probst LFD, Campos CEM, Carreño NLV, Moreira MA. A novel synthetic route for magnesium aluminate (MgAl$_2$O$_4$) particles using metal–chitosan complexation method. *Chemical Engineering Journal*. 2012;193-194:211-214. http://dx.doi.org/10.1016/j.cej.2012.04.054

34. Jacobsen CJH, Madsen C, Houzvicka J, Schmidt I, Carlsson A. Mesoporous zeolite single crystals. *Journal of the American Chemical Society*. 2000;122(29):7116-7117. http://dx.doi.org/10.1021/ja000744c

35. Stringhini FM, Mazutti MA, Dotto GL, Jahn SL, Cancelier A, Chiavone-Filho O, et al. Photocatalytic activity of $ZnAl_2O_4$ spinel for Procion red degradation under UV irradiation. *Latin American Applied Research*. 2015;54:51-55.

36. Anchieta CG, Dotto GL, Mazutti MA, Kuhn RC, Collazzo GC, Chiavone-Filho O, et al. Statistical optimization of Reactive Red 141 removal by heterogeneous photo-Fenton reaction using $ZnFe_2O_4$ oxide prepared by microwave irradiation. *Desalination and Water Treatment*. 2015;57(33):15603-15611. http://dx.doi.org/10.1080/19443994.2015.1070761

37. Brasil. Ministério do Meio Ambiente. Conselho Nacional do Meio Ambiente (CONAMA). *Resolução n. 430, de 13 de maio de 2011*. Available from: <http://www.mma.gov.br/port/conama/res/res11/propresol_lanceflue_30e31mar11.pdf>. Access in: 4/10/2016.